A μ-synthesis based control for compliant maneuvers

Yutaka Uchimura* and **H. Kazerooni****

*Kajima Technical Research Institute,
Tobitakyu, Chofu-shi, Tokyo 182, JAPAN
E-mail: uchi@katri.kajima.co.jp

**Mechanical Engineering Department
University of California at Berkeley
Berkeley, CA 94720, USA
kazeroon@newton.berkeley.edu

ABSTRACT

This paper presents a controller design based on μ synthesis for compliant maneuvers, which enables a robust force feedback without using a force sensor. The controller maintains robust stability against uncertainties existing in both environment and human dynamics, which contributes to dexterous manipulation.

The controller described here is implemented on the human power extender, which is worn by a human and amplify the human's physical strength, while the human's intelligence remains as the central control system for manipulation.

1 INTRODUCTION

Recently, with the progress of computers, robot manipulators have obtained some abilities of perception and judgement. However, it still remains a dream that robots have the same or more flexible intelligence than humans. In the meantime physical ability of a robot manipulator is superior in such cases as carrying heavy loads. To benefit from the physical advantage of robots and the intellectual advantage of humans, the human extender was studied [1].

The human power extenders are a class of robots, which are worn by a human and amplify the human's physical strength, while the human's intelligence remains as the central control system for manipulation. The human transfers his/her commands to the extender via the contact forces between the human and the extender. For the sake of better dexterity, the extender should also transfer to the human a scaled-down value of the actual external forces, and then the human "feels" them during manipulations. To achieve this, the force, which interacts between the environment and the extender, has to be sensed.

A force sensor is typical answer, but it is possible to extract only the external force if the exact model of the system is obtained. Due to the existence of nonlinearlities or unmodeled dynamics, the exact model may not be obtained. But it can still be beneficial to let the human operator feel the interactive force as long as the estimated force maintains some degree of accuracy. For this reason, we develop an algorithm which estimates the external forces using input voltage to the actuators and output position from encoders. This force information feeds back to the operator at some scaled down ratio. In another word, the operator's force is amplified in accordance with this ratio. The ratio should maintain the same value as long as the task is same. This is one of the goals for designing a extender control system.

Meanwhile, the control system is subjected to many uncertainties such as human dynamics and unknown environments. The extender must be stable against these various uncertainties. In fact, the performance goal of maintaining the force amplification ratio and stability against uncertainties contradicts each other. Therefore we must design the controller using a criterion, which optimize this trade-off. μ-synthesis is one of the most powerful theories especially for systems which involves independent uncertainties. To take advantage of it, the controller was designed base on this theory.

Section 2 describes the modeling of the extender system and states the problem, which concerns the stability and performance. It also discusses the modeling of human arm. In section 3, we discuss an algorithm to estimate an external force without a force sensor. It also discusses viscous friction at low frequencies and static friction that deteriorate the accuracy of the estimation. Section 4 presents the controller design procedure and experimental results.

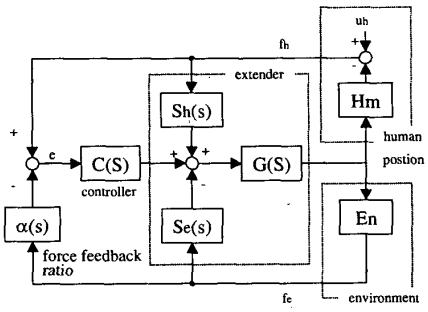

Figure 1: The overall block diagram for the extender

2 MODELING OF THE SYSTEM

The whole dynamics of the human power extender is coupled with the dynamics of the human, environment and the actuator, which are combined in Fig.1. The system mainly involves two loop systems; the human dynamics loop and environmental loop. The upper half of Fig.1 represents the human dynamics loop, which includes the force produced by the human arm impedance,H_m, and intentional forces generated by human's nerve system. The latter force, u_h, is a source for maneuvering the actuator. The force imposed on the actuator,f_h, is the difference between these two forces, which is measured for the controller. The lower half loop represents the dynamics of the environment. It is produced as a result of interaction with the external environment such as contact forces or gravity forces due to the weight of a load. The force,f_e, generated by the impedance of the dynamics, E_n, is also imposed on the actuator. This force is to be estimated by the algorithm which is described in later section.

2.1 Performance

Maneuvering the human arm from one point to another point can be a position servo problem. However, it is impossible to measure the exact position in 3D space where a human would like to move his arm in the

0-7803-5731-0/99$10.00 ©1999 IEEE

next moment. The only thing we can do is to measure the force difference between the human's intentional force and the resistance force due to impedance of the human. At the moment when the human does not want to move his/her arm, zero signals come out. One possible design method of the controller is to place a double integrator whose initial state is a starting position, then input the integrated signal to the position servo controller. However, this should be avoided because the controller is to be implemented on a digital computer. Converting from continuous time integrator to discrete time will result in integration error. Another possible solution is to consider the system as a regulator problem. Now we define performance of the system; to minimize the human's force measured by a sensor. The controller works to keep the measured force zero, which causes the actuator to move along with the human motion. This design scheme is more preferable and has better performance.

Without any interaction with an environment, the specification of the system design is to let the actuator move along with human motion without stress. This will be achieved by attenuating disturbances existing in the actuator such as frictions. However, once the actuator comes into a contact with the external environment, such a performance goal sometimes leads to an unexpected result. Pushing a pin into a hole is a well known example. Under a constrained environment, the human needs to feel the interaction effect from the environment. The force feedback ratio α in Fig.1 takes such a role in the system, which lets designers choose the appropriate performance for the actuator. The larger α is, the more the human feels the interaction. Consequently, the specification of performance is defined in (1)

$$Minimize(f_h - \alpha f_e) \quad (1)$$

2.2 System design based on μ-synthesis

Exact dynamic models for the system are difficult to produce because of uncertainties in the human dynamics, environments and the actuator. The human arm dynamics change with each human and also in one person over time. Moreover, unmodeled dynamics also involves nonlinearly. Uncertain environment may change even more drastically, because the extender has to be always stable both with and without contact. The stiffness of the environment may change from nothing to a very large value. Such perturbations can't be negligible nor be dealt with as unmodeled disturbances.

Several studies about the extender's stability had been made based on small gain theory and derived a sufficient condition [1][2]. They also deal with performance of the system. However, they just show a sufficient condition for the performance and stability. H_∞ synthesis may be a solution for the theoretical procedure of designing a controller. However it will just design a very conservative, sufficient controller for the extender system which has multiple uncertainties. One of the main reasons of this is that the uncertainty of human and environment are independent. These uncertainties should be dealt with separately, i.e. these are to be represented as a structured singular value.

μ-synthesis which can deal with such a system that has multiple independent uncertainties and designs a controller for optimal worst-case performance in the face of plant uncertainties. Associating with weight function performance can be dealt with as a perturbation. However, it is difficult to compute the structured singular value analytically [4], therefore we employed D-K iteration method to obtain the upper and lower value of the structured singular value. In the actual system design of the extender, these two values were very close, therefore the obtained controller must be almost optimal. Controller design procedure is described in a later section.

2.3 Modeling of the human arm

This section describes the dynamic behavior of the human arm. A simplified version of human arm dynamics is already shown in Fig.1. The force imposed by the human arm on the extender results from two inputs. The central nerve system and the motion of the extender forms issue the first input the second input. These two forces can be translated as active force and passive force respectively. If the extender is stationary, the force imposed on the extender is only from the active force. However, if the extender moves, the force imposed on the extender is not only from the active force but also from the passive force. It assumed that the specified form of active force is not known other than that it is the human's intention to move the extender. It may help to illustrate the passive force by imagining that the human is sleeping. The passive force is produced by human arm impedance, which can be modeled as a spring / mass / damper system.

The model may change depending on configuration, therefore the model delivered here approximates an experimentally verified model at a configuration in the neighborhood of Fig.2, which is a typical configuration when operating the extender.

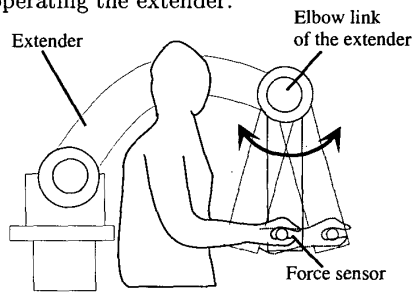

Figure 2: Human experiment overview

For the experiments, an examinee's hand was placed on the grip connected on the force sensor, then the extender was moved along the sinusoidal velocity command. The maximum magnitudes of sinusoidal commands had been set to the same value. Fig.3 shows experimental results of male and female examinee. Horizontal axis is frequency of velocity (rad/sec). Vertical axis is magnitude of the measured force in db form (Nsec/m). At low frequency, the spring factor is dominant and the middle convex part represents dumping coefficient. The inclining curve at high frequency is due to mass effects. By applying the least square method on the data at each frequency, damping and mass were obtained with small standard deviations. However, spring was not. These results show that the human spring factor does not have a linear aspect, even so it must have a certain limited value. To estimate the maximum value of spring factor, we conducted simple 3rd order force feedback system composed of the actuator and 1st order force sensor. In this system, only the spring factor can destabilizes the system. In this experiment, the examinee just holds the bar then we increased proportional gain. At the limit of gain or

phase margin system goes unstable. Based on several experiments, the best estimate for the nominal model of human's arm dynamics is presented by

$$Hm = 2.5s^2 + 50s + \frac{30s}{s+0.2}(N/m) \quad (2)$$

Fig.4 shows frequency responce of (2).

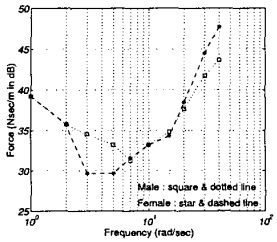

Figure 3: Experimental results on human arm

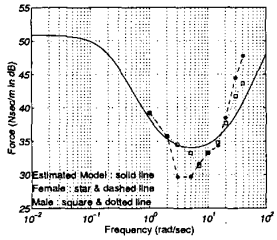

Figure 4: Frequency responce of nominal model

3 ESTIMATION OF THE EXTERNAL FORCE

3.1 The estimation procedure

For simplicity, we discuss only one of the links of the extender, whose block diagram is depicted in Fig.5

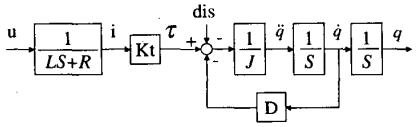

Figure 5: The dynamics of a link

Notations are as follows: u is input voltage to the motor, i is current, K_t is torque coefficient, N is a speed reduction ratio, τ is the torque , D is viscous friction, J is the inertia both of the link and the motor, L is the inductance, R is the resistance and q is the rotational angle. *dis* stands for disturbances which are not defined explicitly in the block diagram such as coulomb frictions, coliolis, centrifugal forces, external forces and model uncertainties.

Coliolis and centrifugal forces are negligible when N is large enough. Also L is very small compared to R, hence we can approximate the dynamics of the link as

$$Eu = J\ddot{q} + D\dot{q} + Mg\sin q + Csgn(\dot{q}) + F_{ex} \quad (3)$$

where E=KtN/R, J is the inertia , D is the gravitational torque and C is coulomb friction. Now we define a vector $\mathbf{X}$=$[J\ D\ Mg\ C]^T$,and $\mathbf{A}$=$[\ddot{q}\ \dot{q}\ \sin q\ sgn(\dot{q})]$, (3) can be rewritten

$$Eu = \mathbf{AX} + F_{ex} \quad (4)$$

$\ddot{q}$, $\dot{q}$, $\mathbf{X}$ and $\sin q$ can be numerically calculated from the measurement set of u and q as a sequence of time responses.

In practe, measured data should be filtered to maintain quality against noise. Therefore (4) is rewritten associated with noise.

$$Eu^* = \mathbf{A}^*X + F_{ex}^* + \omega \quad (5)$$

where u^*,A^*,F_{ex}^* are filtered values and w is noise. Since E can be known from the specification of motor or experimental analyses, A^* can be estimated by X from the measurement data when F_{ex}=0. Numbers of least square mean method algorithms were already studied and had come into wide use [3]. Among them, we used Potter Algorithm, which turned out to be more accurate and stable than Kalman by the experiment.

Once the external force works on the manipulator, subjected external force F_{ex} is measured as

$$\hat{F_{ex}} = Eu^* - \mathbf{A}^*\hat{X} + \omega_e \quad (6)$$

where $\hat{X}$ is estimated parameter vector.

3.2 Frictions at low velocity

In the practical system, position is obtained from an encoder, which gives quantized (digital) values. This causes a numerical differential operation to generate jaggy oscillations along $(q) = 0$ and the coulomb friction term $Csgn(\dot{q})$ switches between $-C$ and C at very high frequency. As a result, estimated external force will be corrupted intolerable with noise. To avoid this, we implement an insensitive area for the sgn function by replacing it to the following function $sw(\dot{q})$.

$$sw(\dot{q}) = \begin{cases} 0 & |\dot{q}| < \delta \\ sgn(\dot{q}) & |\dot{q}| \geq \delta \end{cases} \quad (7)$$

where $\delta > 0$ determines the range of insensitivity.

At the moment when velocity is zero, a static friction arises instead of coulomb friction.

Even though the maximum magnitude of the static force is known, the static force can not be estimated accurately, because the static friction changes in accordance with the sum of all other forces. If $\dot{q}$ is zero, the static friction force F_s is defined as

$$F_s = Eu + Mgsin(q) + F_{ex}; \quad |F_s| \leq F_s^{max} \quad (8)$$

Therefore the estimated external force based on the procedure described above may have an error bounded by $|F_s^{max}|$.

Now suppose a force servo control system as shown in Fig.6. When F^{ref}=0, the actuator is required not to move). However $\tilde{F}_{ex}$ is not always zero due to the estimation error. As a result, the link will start to move.

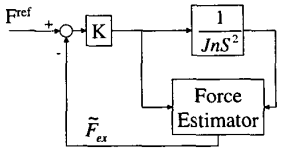

Figure 6:

Essentially, what we proposed is to construct the reverse system dynamics. Static friction can be modeled as a dead zone depicted in Fig.7. Therefore we also need a dead zone located at the end of the reverse system.

The revised estimation algorithm when $sw(\dot{q}) = 0$ is shown in (9):

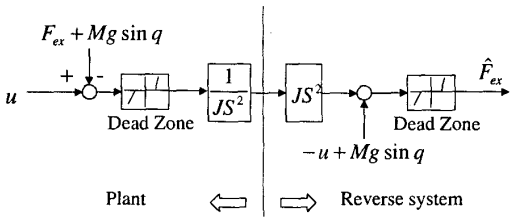

Figure 7:

$$\tilde{F_{ex}} = \begin{cases} -F_m & |F_m| > F_s^{max} \\ 0 & |F_m| \leq F_s^{max} \end{cases} \quad (9)$$

F_m=$Eu + Mgsinq$

3.3 Experimetal results

3.3.1 Model identification The experiments are conducted using the last link (elbow link) of the extender for parameter. We executed identification with various input command signals into the actuator. Among them, a chirp signal with DC offset was expected to be most reliable, because they contain contributions from a specified frequency range. The signal possesses (nearly) uniform frequency components between 0(rad/sec) and 100(rad/sec). A time response plot of the signal appear in Fig.8. The result of identification is shown in Table 1.

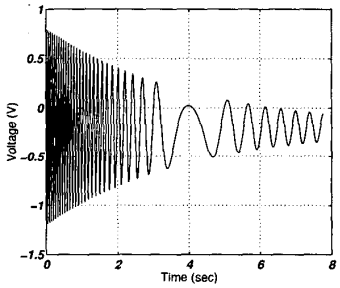

Figure 8: Input signal for identification

Table 1: Identification result

J (Nms^2/rad)	D(Nms/rad)	C(Nm)	Mg(Nm/rad)
4.48	23.2	14.54	35.01

(* $K_tN/R = 118Nm/V$)

3.3.2 Estimation of external force In order to verify the reliability of identified dynamics, we conducted experiments as shown in Fig.9. The external force is emulated by a tension spring which is connected between the base of the extender and end of the elbow link. The actuator is controlled to follow a sinusoidal velocity command, while stretching the spring. Fig.10 shows the experimental result. The magnitude of estimated force is fairly accurate, while a phase delay is observed. The low pass filtering used in the force estimation process causes the phase delay. Excessive delay will cut out the stability margin of the system, therefore in the implementation to the real plant, even the controller will be designed by the robust control theory, and one should carefully design the filter.

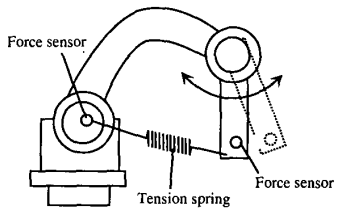

Figure 9: Experimental configulation

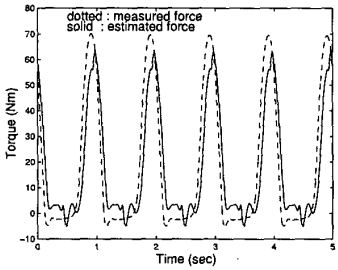

Figure 10: Estimation results

4 CONTROLLER DESIGN AND EXPERIMENTAL VERIFICATION

4.1 Controller design

The block diagram of the closed loop system is shown in Fig.11. The closed loop system includes the feedback structure of elements associated with the uncertainty models and performance objectives. The design objective of the controller is to stabilize the system against uncertainties of actuator, human and environmental dynamics while optimizing performance.

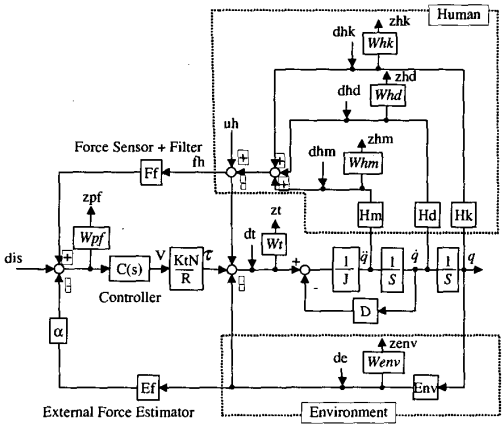

Figure 11: Block diagram with uncertainties

4.2 Nominal models and uncertainties

Actuator

Nominal model of the actuator is derived form the result of identification which are described in section 3.

$$P_m(s) = \frac{26}{s(s+6)} \quad (10)$$

Uncertainty of the actuator was modeled as a multipicable uncertainty with a weighting function which is chosen as follows

$$W_t(s) = \frac{100s^2 + 2656s + 3.6 \times 10^7}{s^2 + 2656s + 3.6 \times 10^8} \quad (11)$$

The uncertainty weight chosen indicates that at low frequencies there is potentially a 10% modeling error, and at high frequencies the model is up to 100 times larger than the nominal model.

Human dynamics

Nominal model of human dynamics is derived from the experimental analysis in section 2

$$H_{nominal}(s) = H_{mn}s^2 + H_{dn}s + H_{kn} \quad (12)$$

where $H_{mn} = 2.5Nsec^2/m$, $H_{dn} = 50Nsec/m$, $H_{kn} = \frac{30s}{s+0.2}(N/m)$. Uncertainty of the human is modeled as multiplicable real parametric perturbations. To normalize the perturbation, the weights are chosen 0.2,0.3,0.3 which indicate that the human's mass, damper and spring may change 20%,30%,30% respectively.

Environment dynamics

Nominal environment is modeled as a spring system. Uncertainty is modeled as a multiplicable complex parametric perturbation whose weight is 1. This assumes the stiffness of the environment will perturb 0 to 200% of nominal value. One should need to notice that complex parametric perturbation assumes that the environment also has a damper whose magnitude will also perturb. Because a complex uncertain parameter is mathematically equivalent to robustness, whose Nyquist plots lie in the disks. Suppose the nominal stiffness of the spring is 5000N/m, the system can exist within the circle with center at 5000 Nm/rad and radius 5000 N/rad.

Robust performance

Robust performance is defined as minimizing the error of difference between the human force and the scaled down external force. This performance will be affected due to disturbances, which comes into just before the error on the block diagram. These disturbances can be noise, external force other than environmental force and/or active forces commanded by the human. W_pf is the weighting function chosen to have a sufficient gain within the human bandwidth. Following equation is a feasible choice of W_pf is shown as follows,

$$W_{pf}(s) = \frac{360}{s^2 + 8.48s + 36} \quad (13)$$

Filters

There are two filters in the system to attenuate noise at the high frequency. One is the filter for the force sensor which measures the human's force. The other one exists in the external force estimation. The filter for the force sensor is chosen as 2nd order Butterworth filter whose cutoff frequency is 50 (rad/sec). The force estimation uses numerical derivatives to obtain acceleration and velocity associated with low pass filters. These filters are also applied to other elements. Therefore total filter order is 4th order low pass filter which is chosen as

$$Ef(s) = \frac{1}{(1/50s + 1)^4} \quad (14)$$

Because these filters are digital filters on the host computer of the extender, therefore we assume no uncertainty.

4.3 Computation of controller and trade-off between stability and performance

Performance is strongly affected by the uncertainties of the plant. In the case of the extender model, the uncertainty of the environment restricts performance most significantly. For this reason, we had to compromise either performance or maximum stiffness of the environment. Such trade-off depends on the purpose of using the extender. In our study, reasonable problem statement is: Achieve less than 10% error for the environment whose nominal value is 12500 N/m, and may change from 0 to 25000 N/m.

The controller is obtained using D-K iteration methods, whose maximum D-scale state order is 5. After 4 D-K iterations a 40 state controller was obtained which achieved a structured singular value μ less than 1. Fig.12 shows frequency response plots of the upper and lower bounds for μ. For the experimental implementation, the controller order was reduced to 12 using truncated balance realizations. The reduced order controller still maintains closed-loop stability and robust performance. Fig(13) shows the bode diagram of the controller.

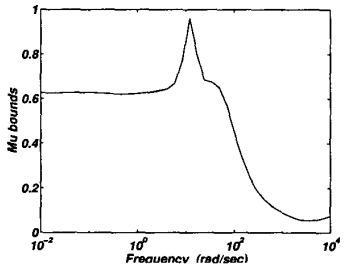

Figure 12: Upper and lower bounds of μ

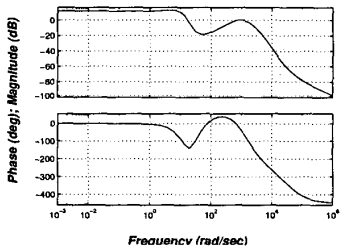

Figure 13: Bode diagram of the controller μ

4.4 Experimental results

The prototype three-degree of freedom electrical extender (Fig.14) is used to verify the stability and performance of the controller implemented system. For the experiment, only the last link from the base (the elbow link) was used. A piezo electric force sensor for measuring the human force is installed near the end of the link. The actuator of the link is composed of a DC brush less motor and a harmonic drive gear with a reduction ratio of 50:1. To emulate the environment two test pieces were employed; a tensional spring whose

stiffness is about 4000N/m and a metal wire whose stiffness is around 20000 N/m. Either of them is set between the base of the extender and the manipulation point near the grip an operator holds (c.f. Fig9). Additionally, another force sensor is mounted on the end of the spring to verify the accuracy of the force estimation.

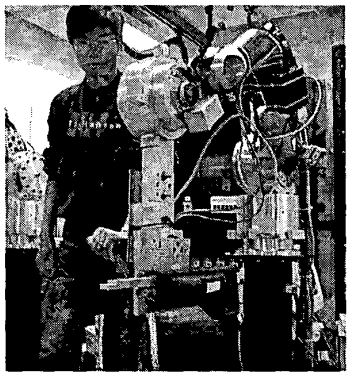

Figure 14: The prototype extender

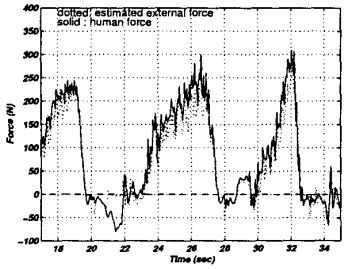

Figure 15: Human / Estimated force (spring)

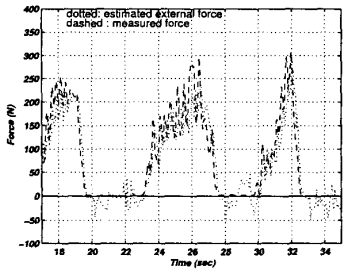

Figure 16: Estimated / Measured force (spring)

Spring environment: force feedback ratio α=0.1

Fig.15 shows the time response of the human force (solid line) and the estimated external force (dotted line) when force amplification filter is set on 0.1,i.e. the human force will be amplified 10 times. For convenience of comparison, the estimated force is magnified at 10 times. Fig 16 shows comparison of the estimated force and measured force (dashed line) to examine the accuracy of estimation.

Wire environment: force feedback ratio α=0.1

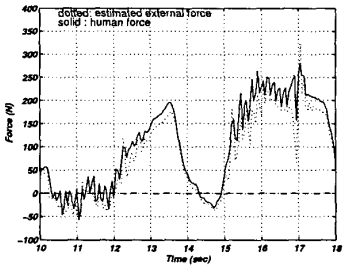

Figure 17: Human / Estimated force (wire)

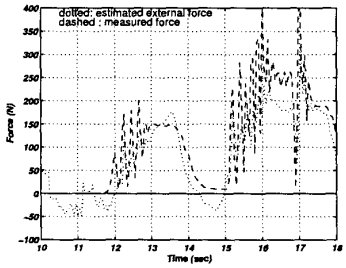

Figure 18: Estimated / Measured force(wire)

Fig 17 shows the time response of measured human force and estimated external force in the same manner as previous case. Fig 18 shows comparison of the estimated force and measured force to examine the accuracy of estimation.

In both cases the estimation stayed within tolerant range while the system was stable and error between the human force and the estimated external force is smaller than 10% of magnitude of human force, which proves that performance requirements were satisfied.

5 CONCLUSION

In this paper, we dealt with a system which is subjected to very uncertain factors: human and environment controller. These independent uncertainties were dealt explicitly base on μ synthesis and less conservative controller was obtained. We also developed a force sensorless control by taking into consideration of nonlinearly such as frictions and gravity force. A scale downed reaction force based on the estimation contributes compliant maneuvers. Finally, through experimental studies on the human power extender robot, stability and performance of the system were verified.

REFERENCES

[1] H. Kazerooni: "Human-robot interaction via the transfer of power and information signals",IEEE Trans. on Systems, Man and Cybernetics , vol.20, 1990

[2] H. Kazerooni,et al: "Modeling human arm movements constrained by robotic systems ", ASME Eng. Dyn. Sys. Control, vol.42 pp 19-24, 1992

[3] G. Bierman: "Factorization methods for discrete sequential estimation", Academic Press, 1977

[4] G.Chen,T.Sugie: "An Upper Bound of μ Based on the Parameter Dependent Multipliers", Proc. of American Control Conference, pp. 2604–2608,1997

[5] "μ-analisis and synthesis toolbox user's guide", Mathworks